ISSN 1063-7834, Physics of the Solid State, 2016, Vol. 58, No. 4, pp. 699–702. © Pleiades Publishing, Ltd., 2016.
Original Russian Text © V.I. Vettegren, I.P. Shcherbakov, R.I. Mamalimov, V.B. Kulik, 2016, published in Fizika Tverdogo Tela, 2016, Vol. 58, No. 4, pp. 681–684.

MECHANICAL PROPERTIES, PHYSICS OF STRENGTH, AND PLASTICITY

Structural Changes in a Heterogeneous Solid (Granite) under Shock Wave Action

V. I. Vettegren*, I. P. Shcherbakov, R. I. Mamalimov, and V. B. Kulik

Ioffe Physical-Technical Institute, Russian Academy of Sciences, ul. Politekhnicheskaya 26, St.Petersburg, 194021 Russia

** e-mail: Victor.Vettegren@mail.ioffe.ru*

Received September 21, 2015

Abstract—The structure of two granite types (plagiogranite and alaskite) before and after shock wave action has been studied by infrared, Raman, and photoluminescence spectroscopy methods. It has been found that the shock wave caused transformation of quartz and feldspar crystals composing these granites into diaplectic glasses.

DOI: 10.1134/S1063783416040302

1. INTRODUCTION

Recently, much progress has been made in the field of solid deformation kinetics under shock wave action [1–3]. The construction of the theoretical model of fracture under shock wave loading was initiated [4]. The first experimental data on the dielectric fracture mechanism were obtained [5–7] due to the development of a setup recording luminescence dynamics with nanosecond resolution. It was found that beams of positively charged ions and electrons are emitted from dielectrics under shock wave action. Simultaneously, dielectrics decay into fragments from several micrometers to several millimeters in size.

In [8], the surface of a quartz single crystal fragment after shock wave action was studied by IR reflectance spectroscopy. It was found that a layer of diaplectic glass, i.e., quartz with extremely strongly distorted lattice, was formed on its surface.

The present work continues the cycle of these investigations. The structure of granite fragments and powders formed after shock wave action is studied.

2. RESEARCH OBJECT AND METHOD

Samples represented parallelepipeds sawed out of two granite types, i.e., plagiogranite and alaskite, by a diamond saw. They contained quartz crystals (30–40 vol %) and two feldspar types, i.e., plagioclase and sandine. The sample size was 10 × 10 × 20 mm. At the sample center, a hole ~1 mm in diameter was drilled, into which copper electrodes spaced by ~4 mm were placed. The setup block diagram is described in [6]. Discharge between electrodes produced plasma [9] consisting of Cu microparticles and atoms. It initiated a shock wave in the quartz sample, which propagated with a velocity of ~6 km/s [6]. Under shock wave action, a plasma jet consisting of positively charged silicon, oxygen ions, and electrons emitted from the sample in ~1 μs. The mechanism of its formation is described in [8]. Simultaneously, the sample decayed into fragments from several micrometers to several millimeters in size.

The structures of granite samples before explosion and their fragments after explosion were studied by infrared (IR), Raman and photoluminescence (PL) spectroscopy methods.

IR reflectance spectra were recorded using an IR-21 Prestige Fourier-spectrometer with an SRM-8000A attachment. The angle of beam incidence on the sample was 10°.

Raman spectra were recorded using a Ramalog-5 spectrometer. The spectra were excited by an Ar^{2+} 16508 (Spectra Physics) argon laser (514.5 nm line). The laser beam, focused into a spot ~30 μm in diameter, was directed on the surface of the sample placed on a subject stage. The backscattered light beam was directed to a monochromator entrance slit using a mirror and a focusing optical system. To more accurately determine the frequencies and shifts of band maxima, the spectra were recorded simultaneously with laser lines whose positions were used as reference points.

PL spectra were recorded at an angle of 10° to the beam of an LGI-21 pulsed laser (3.68 eV line). The size of the area under study on the sample surface, controlled by the focused laser beam size, was 2 mm. The spectra were recorded using an AvaSpec-ULSi2048L-USB2 OEM fiber-optic spectrometer. The measured band intensity was normalized to the intensity of the laser beam reflected from the surface.

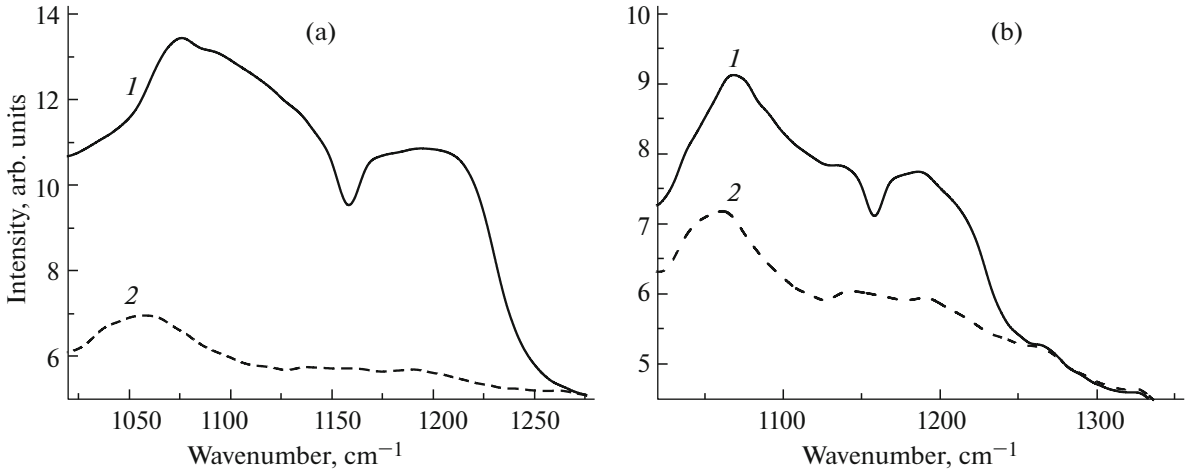

Fig. 1. IR reflectance spectra of (*1*) two granites before explosion and (*2*) their fragments after explosion: (a) plagiogranite and (b) alaskite.

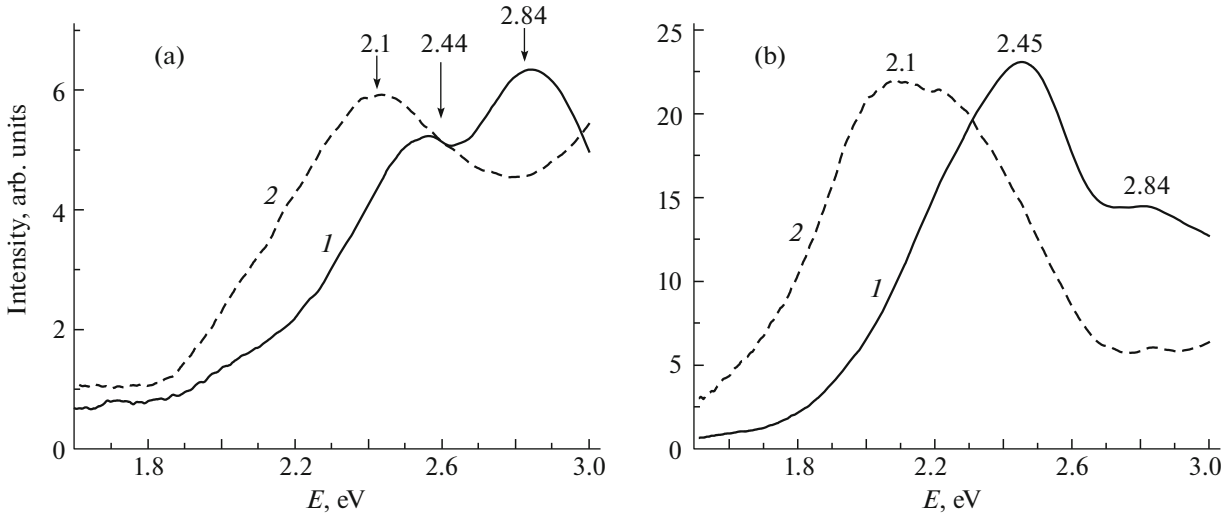

Fig. 2. PL spectra of (*1*) granite samples and (*2*) powders formed of them after shock wave action: (a) plagiogranite and (b) alaskite.

3. MEASUREMENT RESULTS AND DISCUSSION

3.1. Infrared Spectroscopy Data

Figure 1 shows the portions of IR reflectance spectra of the surface of initial granite samples and fragments with linear sizes of ~3 × 4 mm before and after shock wave action.

We recall that the oscillation amplitude of the electric vector of IR radiation is damped exponentially from the sample surface to the depth. The depth h at which it decreases by a factor of $e \approx 2.7$ (e is the base of the natural logarithm) and the radiation intensity decreases by a factor of $e^2 \approx 8$ corresponds to the effective surface layer thickness information on which is carried by the reflectance spectrum. This thickness is calculated by the formula [10]

$$h \approx 1/4\pi\nu k, \quad (1)$$

where k is the absorbance and ν is the radiation frequency. Calculations showed that the effective thickness of the surface layer was ~0.1–0.2 μm.

The spectra contain two maxima attributed to stretching vibrations of quartz and feldspar (plagioclase and sandine) lattices [11–14]. We can see that the intensity of maxima after shock wave action decreases by a factor of ~1.5–2. Simultaneously, the characteristic minimum in the region of 1150 cm^{-1} disappears. This means that the quartz and feldspar

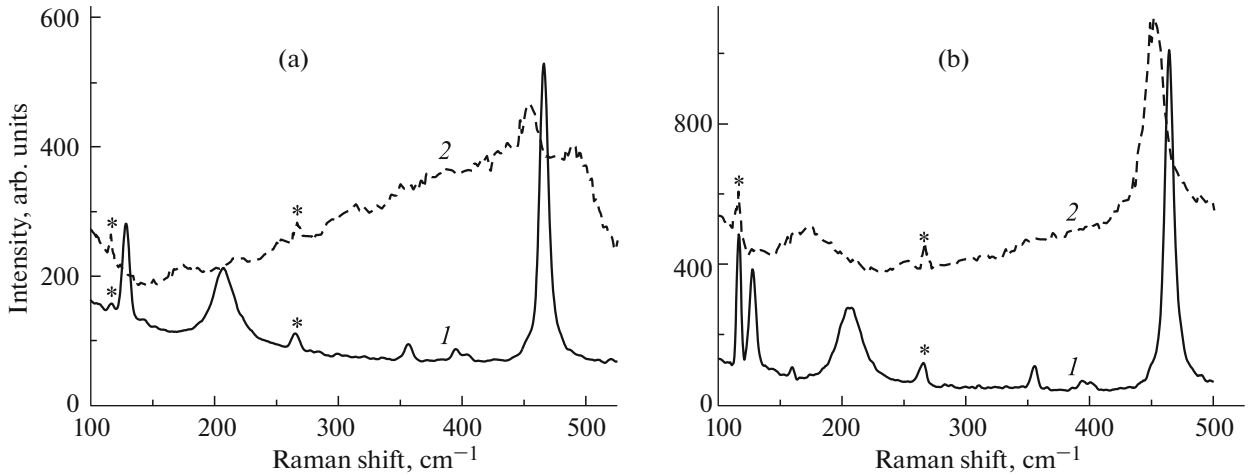

Fig. 3. Raman spectra of (*1*) quartz in (a) alaskite and (b) plagiogranite and (*2*) its powder formed under shock wave action. Asterisks indicate laser emission lines.

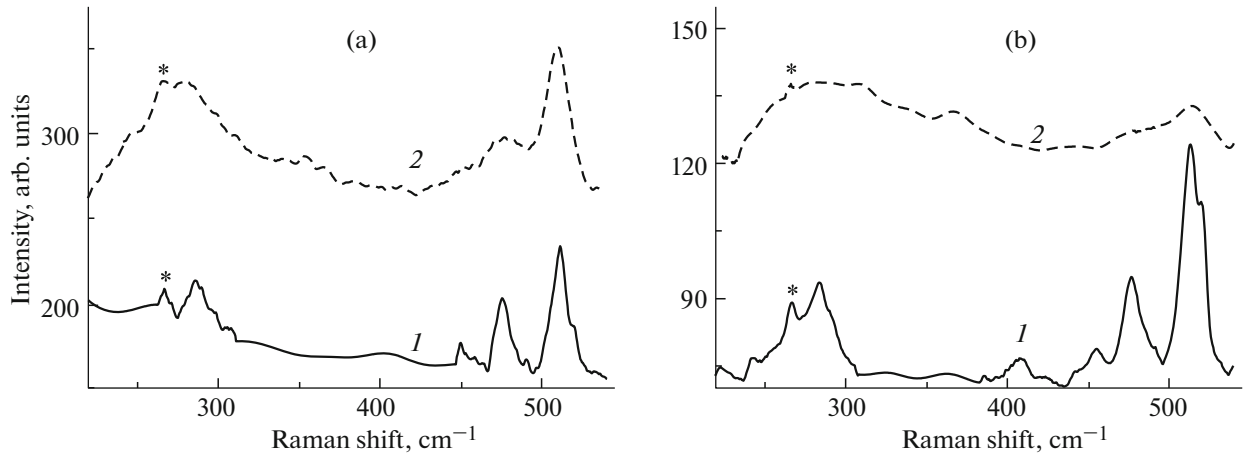

Fig. 4. Raman spectra of sandine in alaskite (a, curve *1*), plagioclase in plagiogranite (b, curve *1*) and (*2*) powders of these feldspars, formed after shock wave action. Asterisks indicate laser emission lines.

lattice is transformed to diaplectic glass, i.e., a material with a strongly distorted crystal structure [15–20].

3.2. PL Spectroscopy Data

Figure 2 shows the PL spectra of initial samples and powders with grain sizes of several dozen micrometers. Before shock wave action, the spectra of both granites contained two bands: 2.44 and 2.84 eV. The first and second bands are attributed to electronic transitions in Mn^{2+} ions and in Al–O^-–Al centers [21]. Under shock wave action, the intensity of the band at 2.84 eV decreases, i.e., the Al–O^-–Al ion concentration decreases. The intensity of the second maximum remains almost unchanged, but its energy decreases by ~0.3 eV, and the width increases. According to [22, 23], these changes are caused by fracture of quartz and feldspar lattices and the formation of diaplectic glasses in their place.

3.3. Raman Spectroscopy Data

Figures 3 and 4 show the Raman spectra of samples before shock wave action and powders with grain sizes of several dozen micrometers, formed after shock wave action.

As noted above, the laser beam diameter is ~30 μm, and linear sizes of the quartz and feldspar crystals in the first and second samples are 2–5 mm and 5–8 mm, respectively [24]. This made it possible to measure quartz and feldspar spectra separately. These spectra are shown in Figs. 3 and 4 (curves *1*).

The powder produced after shock wave action was sorted by color into three fractions. The first fraction,

i.e., the "white" one, represented quartz grains, the second "red" fraction represented sandine grains, and the third dark gray fraction represented plagioclase grains. The spectra of powders are shown in Figs. 3 and 4 (curves *2*). We can see that the narrow bands attributed to vibrations of lattices of these minerals disappear in the spectra of all samples exposed to shock waves; in their place, broad maxima corresponding to variations of diaplectic glasses appear [25, 26].

Thus, all three spectroscopy methods showed that the crystal structure of quartz and feldspar incorporated in granite is transformed to diaplectic glasses.

4. CONCLUSIONS

Under shock wave action, the quartz and feldspar lattice is destructed and diaplectic glass is formed in its stead.

ACKNOWLEDGMENTS

This study was supported by the Russian Foundation for Basic Research (project no. 13-05-00011-a).

REFERENCES

1. V. V. Adushkin and A. A. Spivak, *Geomechanics of Large-Scale Explosions* (Nedra, Moscow, 1993) [in Russian].
2. G. I. Kanel, S. V. Razorenov, and V. E. Fortov, *Shock-Wave Phenomena and the Properties of Condensed Matter* (Springer-Verlag, New York, 2004).
3. B. E. Fortov, Phys.—Usp. **50** (4), 333 (2007).
4. G. A. Malygin, S. L. Ogarkov, and A. V. Andriyash, Phys. Solid State **55** (4), 780 (2013); G. A. Malygin, S. L. Ogarkov, and A. V. Andriyash, Phys. Solid State **57** (9), 1818 (2015).
5. V. I. Vettegren, A. V. Voronin, V. S. Kuksenko, R. I. Mamalimov, and I. P. Shcherbakov, Phys. Solid State **56** (2), 317 (2014).
6. V. I. Vettegren, I. P. Shcherbakov, A. V. Voronin, V. S. Kuksenko, and R. I. Mamalimov, Phys. Solid State **56** (5), 1018 (2014).
7. V. I. Vettegren, I. P. Shcherbakov, V. S. Kuksenko, and R. I. Mamalimov, Phys. Solid State **56** (9), 1828 (2014).
8. V. I. Vettegren', V. S. Kuksenko, I. P. Shcherbakov, and R. I. Mamalimov, Phys. Solid State **57** (12), 2458 (2015).
9. K. B. Abramova, I. P. Shcherbakov, and A. I. Rusakov, Tech. Phys. **44** (2), 259 (1999).
10. M. Born and E. Wolf, *Principles of Optics*, 2nd ed. (Pergamon, Oxford, 1964).
11. M. Etchepare, L. Merian, and J. Smetankine, J. Chem. Phys. **60**, 1873 (1974).
12. K. Iishi and H. Ymaguchi, Am. Mineral. **60**, 907 (1975).
13. S. Shimoda and J. E. Brydon, Clays and Clay Miner. **19**, 61 (1971).
14. J. L. Bishop, M. D. Lane, M. D. Dyar, and A. J. Brown, Clays and Clay Miner. **43**, 35 (2008).
15. J. L. Bishop and E. Murad, J. Raman Spectrosc. **35**, 480 (2004).
16. H. Schneider, Meteoritics **13** (2), 227 (1978).
17. F. Langenhorst, Bull. Czech Geol. Surv. **77**, 265 (2002).
18. M. Chen, C. Koeberl, W. Xiao, X. Xie, and D. Tan, Meteorit. Planet. Sci. **46** (5), 729 (2011).
19. J. J. Wackerle, Appl. Phys. **33**, 922 (1962).
20. M. G. C. O. Goltrant, H. Leroux, J.-C. Doukhan, and P. Cordier, Phys. Earth Planet. Inter. **74** (3–4), 219 (1992).
21. J. Götze, M. Plötze, and D. Habermann, Mineral. Petrol. **71**, 225 (2001).
22. D. Haymann and F. Hörz, Phys. Chem. Miner. **17**, 38 (1990).
23. M. Kayama, A. Gucsik, T. Nakazato, H. Nishido, and K. Ninagwa, Antarctic Meteorites **XXXII**, 28 (2009).
24. V. I. Vettegren, V. S. Kuksenko, and I. P. Shcherbakov, Phys. Solid State **54** (7), 1425 (2012).
25. P. F. McMillan and G. H. Wolf, Phys. Chem. Miner. **19**, 71 (1992).
26. D. Heymann and F. Horz, Phys. Chem. Miner. **17**, 38 (1990).

Translated by A. Kazantsev